CHEMISTRY OF MATERIALS

pubs.acs.org/cm

Article

Stereocomplex Nanocomposite Switch Based on Dynamic Helical Polymer-Gold and Silver Nanoparticle Hybrid Materials

Manuel Núñez-Martínez, Emilio Quiñoá, and Félix Freire*

Cite This: *Chem. Mater.* 2023, 35, 4865−4872

Read Online

ABSTRACT: Controlled ON/OFF stereocomplexation of dynamic helical polymer-metal nanoparticle nanocomposites—poly(phenylacetylene)-MNP nanocomposites (M = Au or Ag)—is presented. These novel hybrid materials can be found either as well-dispersed metal nanoparticles (MNPs) (stereocomplex OFF) or as fiber-like aggregates (stereocomplex ON) with the metal nanoparticles distributed along the material. A stereocomplex-MNP nanocomposite is formed by the interaction of two complementary and enantiomeric helical polymer-MNP nanocomposites [Poly-(*R*)-**1**-M_1NPs/poly(*S*)-**1**-M_2NPs (M_1 = M_2 or $M_1 \neq M_2$; M = Au, Ag)]. Interestingly, by using dynamic helical polymers, i.e., poly(phenylacetylene)s (PPAs), as coating agents of the metal nanoparticles, it is possible to tune the secondary structure of the polymer—elongation and/or compression—a fact that can trigger the formation/disruption of the stereocomplex. Moreover, the stereocomplexation of these nanocomposites can be controlled in a reversible way (ON/OFF) by playing with the supramolecular interactions that keep the two enantiomeric and complementary helices together, such as hydrogen bonds.

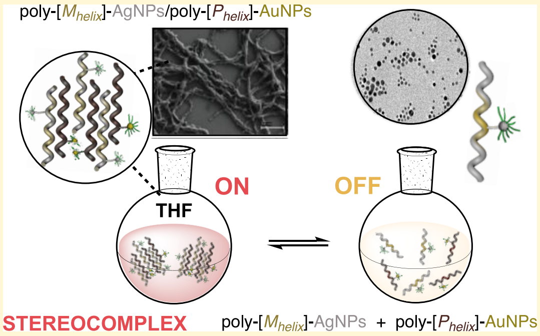

1. INTRODUCTION

Metal nanoparticles (MNPs) have been exploited during the last decades by the scientific community due to their applications in fields such as theranostic,[1,2] sensing,[3] or catalysis.[4,5] To apply these materials in different fields, and work under different conditions—solvent, temperature, etc.—it is necessary to decorate the NMP surface with an appropriate coating, usually an organic molecule. Thus, in the literature, it is possible to find research articles dealing with the functionalization and postfunctionalization of the MNP surface,[6] which include helical natural (DNA or peptides) and nonnatural macromolecules (helical polymers).[7−10]

The use of nonnatural macromolecules such as dynamic helical polymers[11−37] as coating agents introduces interesting properties into the nanocomposite, such as the ability to modify the macromolecular chirality of the coating—screw sense—or the stretching degree—helical pitch—by changing the environmental conditions, e.g., temperature, solvent, pH or by adding external agents, e.g., metal ions, anions, and chiral additives, among others.[38−42]

From previous studies, it is known that the dynamic behavior of the helical polymer in a dynamic helical polymer-MNP nanocomposite can be altered by the binding strength between the polymer and the MNP.[9] Thus, in the case of using PPAs bearing a thiol or thioether group as linking groups to the MNPs, it is necessary to prepare a copolymer due to the poor solubility of the homopolymers containing thiol or thioether groups in the monomer repeating units.[7,10] In the case of preparing a copolymer, it is necessary to consider all the chiral communication mechanisms that can emerge between the two components. Thus, when the copolymer is made up of two chiral monomers, a "Chiral Accord" or "Chiral Coalition" effect should occur between monomers to preserve the dynamic behavior and the screw sense excess in the copolymer, whereas if one of the monomers is chiral and the other nonchiral a "Sergeants and Soldiers" effect should be triggered within the copolymer series.

On the other hand, if a supramolecular interaction with an amide—the MNP type—is used to link the two components of the nanocomposite, homopolymers can be used, although the presence of certain functional groups in the monomer repeating unit or the use of polar solvents may affect the correct formation of the desired hybrid materials.[8] Hence, to design correctly a dynamic chiral nanocomposite, it is necessary to consider the functional groups present in the homopolymer/copolymer and the environmental conditions where the nanocomposite will be used.

In this work, we aim to demonstrate that dynamic helical polymer-MNP nanocomposites can be used not only to prepare nanomaterials with a dynamic chiral coating, but also

Received: April 17, 2023
Revised: May 28, 2023
Published: June 9, 2023

https://doi.org/10.1021/acs.chemmater.3c00912
Chem. Mater. 2023, 35, 4865−4872

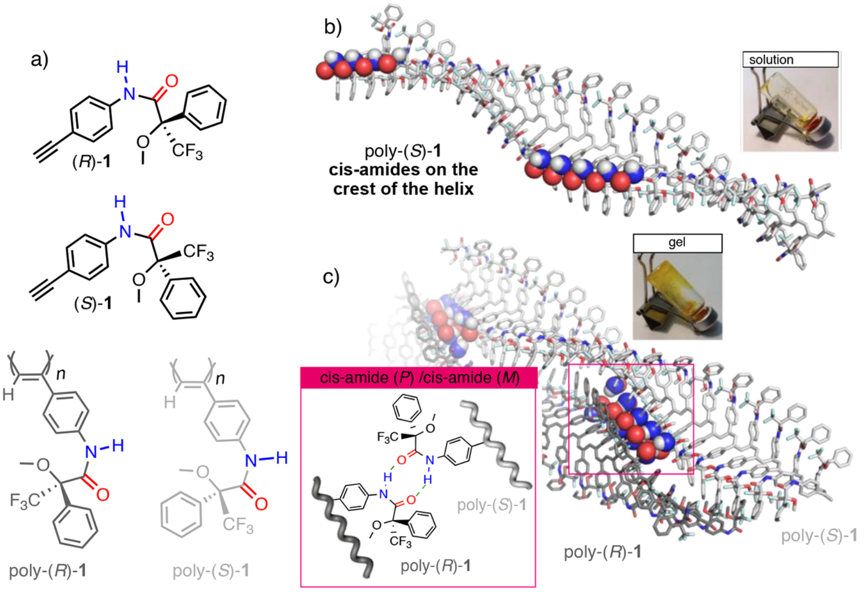

Figure 1. Chemical structure of (a) monomers (*R*)- and (*S*)-**1**; polymers poly-(*R*)- and (*S*)-**1**. (b) 3D-model of poly-(*S*)-**1** showing a *cis*-configuration of the amide groups. Picture of a THF solution of poly-(*S*)-**1**. (c) 3D model of the poly-**1** stereocomplex, highlighting the *cis*-amide/*cis*-amide supramolecular interactions between complementary helices. Picture of a poly-(*R*)-**1**/poly-(*S*)-**1** stereocomplex gel in THF.

to introduce additional properties into the material associated with the helical structure of the coating agent, such as the formation of stereocomplexes. Stereocomplexes are supramolecular aggregates formed by the interaction of complementary stereoregular polymers with different properties to the parent homopolymers.[43] Attending to the composition of the polymers, two different types of stereocomplexes can be formed: homostereocomplexes, formed from enantiomeric homopolymers and heterostereocomplexes, generated by the interaction between polymers with structurally different and opposite absolute configuration, e.g., Poly-(*D*)- and Poly-(*L*)-(Lactic acid) (PLA), or different tacticities, e.g., syndiotactic and isotactic Poly(methylmetacrylate)s [*st*- and *it*-PMMA].[44−49] These stereocomplexes have also been used to prepare nanocomposites with graphene oxide (GO), clay, carbon nanotubes, cellulose nanocrystals, silica, or metal nanoparticles.[46−50]

Likewise, in these stereocomplexes—Poly-(*D*)-PLA/Poly-(*L*)-PLA; *st*-PMMA/*it*-PMMA—the helical structure adopted by the polymers cannot be tamed by using external stimuli. Moreover, the interaction between enantiomeric or complementary helices is attributed to the presence of weak supramolecular interactions such as Van der Waals forces or hydrogen bond interactions, although the mechanism of formation is still unclear.[45]

Here, our goal is to prepare stereocomplexes from dynamic helical polymer-MNP (M = Ag or Au) nanocomposites. Thus, by playing with different external stimuli it is possible to tune the helical structure of the helical polymer-MNP nanocomposite and, therefore, to selectively activate the formation/disruption of the stereocomplex-nanocomposite.

Our group has experience in the preparation of stimuli-responsive stereocomplexes by interaction of helically complementary poly(phenylacetylene)s (PPAs) obtained from polymerization of the 4-ethynylanilides of (*R*)- and (*S*)-α-methoxy-α-trifluoromethylphenylacetic (i.e., (*R*)-**1** and (*R*)-**2**) yielding poly-(*R*)-**1** and poly-(*S*)-**1**, respectively (Figure 1a).[45] In this case, the stereocomplex is formed by supramolecular interactions between complementary helices that bear *cis* amide bonds at their peripheries, leading to the formation of supramolecular fiber-like aggregates that at higher concentrations result in gels (Figure 1b,c). Modification of the *cis*—*trans* amide conformation at the pendants by solvent polarity or disrupting the hydrogen bond interactions by increasing temperature or addition of donor solvents (e.g., MeOH) allows the controlled formation and cleavage of the stereocomplexes.[51] Therefore, Poly-**1** is a great candidate to create a stimuli-responsive stereocomplex PPA-MNP (M = Au, Ag) nanocomposite. However, in previous work, we found that poly-**1** does not form stable poly-**1**-MNPs (M = Au, Ag) through supramolecular anilide-MNP interactions.[8] The presence of a CF_3 group in the pendant deactivates the donor behavior of the anilides and thus their ability to interact with the MNPs.[8]

To overcome this problem and prepare stereocomplexes based on Poly-**1** nanocomposites [Poly-(*R*)-**1**-MNPs/poly(*S*)-**1**-MNPs (M = Au or Ag)], a thiolated comonomer must be introduced into the Poly-**1** chain, to connect the dynamic helical polymer to the MNPs. The resulting copolymer must maintain the helical properties and, therefore, the stereocomplexation ability of poly-**1** unaltered (Figure 1).

2. RESULTS AND DISCUSSION

Monomer **2**, consisting of 11-mercaptoundecanoic acid 4-ethynylanilide, was designed and synthetized as an achiral thiolated monomer (see SI for synthetic details). Next, monomer **2** was copolymerized with (*R*)- and (*S*)-**1** (see SI for synthetic details) using an Rh(I) catalyst to form poly-[(*R*)-$\mathbf{1}_{1-r}$-*co*-$\mathbf{2}_r$] and poly-[(*S*)-$\mathbf{1}_{1-r}$-*co*-$\mathbf{2}_r$] with r in the range of 0.01−0.03 (Figure 2 and SI for synthetic details). Thus, three different copolymers were generated for each enantiomeric series—poly-[(*R* or *S*)-$\mathbf{1}_{0.99}$-*co*-$\mathbf{2}_{0.01}$] (M_w = 308,708), poly-[(*R* or *S*)-$\mathbf{1}_{0.98}$-*co*-$\mathbf{2}_{0.02}$] (M_w = 277,477), and poly-[(*R* or *S*)-$\mathbf{1}_{0.97}$-*co*-$\mathbf{2}_{0.03}$] (M_w = 296,729)—(Figure 2a).

Chiroptical studies show that the ECD traces obtained for the different copolymers are quite like those obtained for their

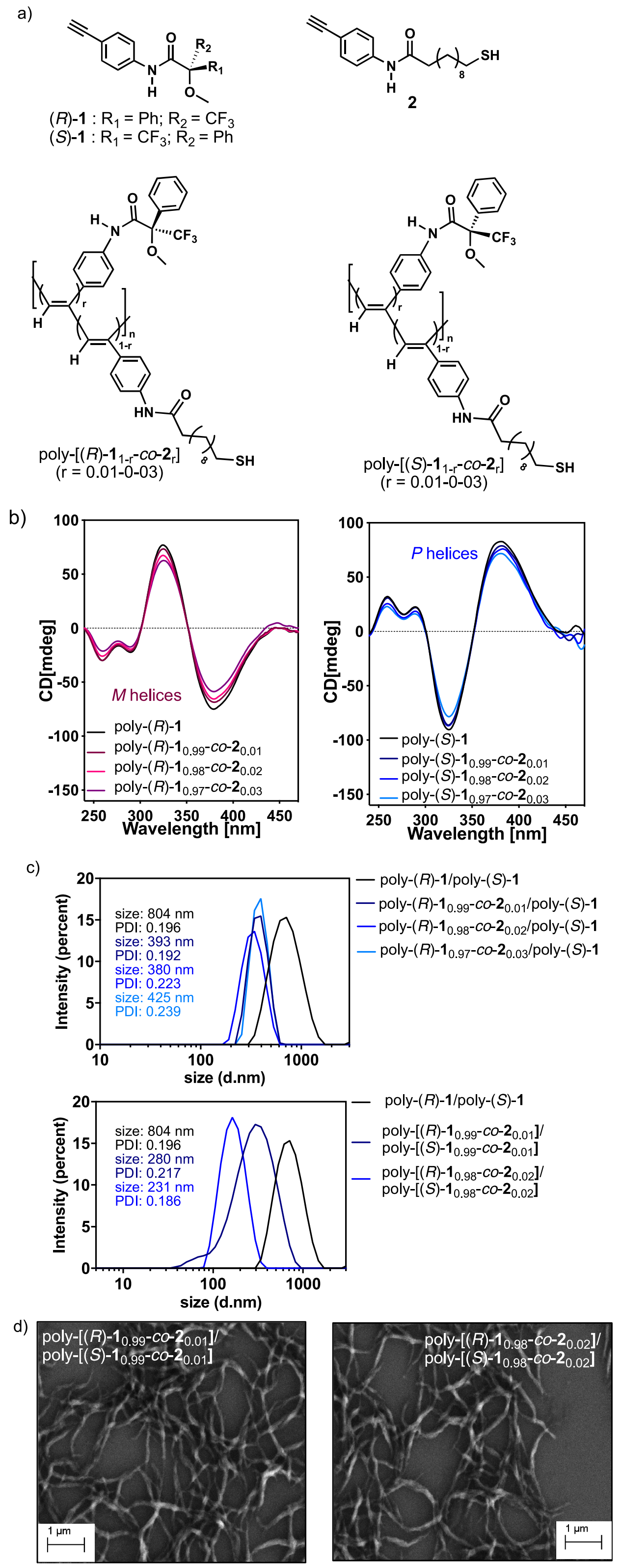

Figure 2. (a) Chemical structure of monomers **1** and **2**, copolymers poly-[(*R*)-$\mathbf{1}_{r}$-*co*-$\mathbf{2}_{1-r}$] and poly-[(*S*)-$\mathbf{1}_{1-r}$-*co*-$\mathbf{2}_{r}$] (r = 0.01−0.03). (b) ECD studies of poly-[(*R*)-$\mathbf{1}_{r}$-*co*-$\mathbf{2}_{1-r}$] and poly-[(*S*)-$\mathbf{1}_{r}$-*co*-$\mathbf{2}_{1-r}$] (r = 0.01−0.03) in $CHCl_3$. (c) DLS studies of poly-(*R*)-**1**/poly-(*S*)-**1** and poly-[(*R*)-$\mathbf{1}_{r}$-*co*-$\mathbf{2}_{1-r}$]/poly-[(*S*)-$\mathbf{1}_{r}$-*co*-$\mathbf{2}_{1-r}$] mixtures (50/50 in THF). (d) SEM images of stereocomplexes formed by poly-[(*R*)-$\mathbf{1}_{r}$-*co*-$\mathbf{2}_{1-r}$]/poly-[(*S*)-$\mathbf{1}_{r}$-*co*-$\mathbf{2}_{1-r}$] mixtures (50/50 in THF) (scale bar: 1000 nm).

corresponding parent homopolymers—poly-(*R*)-**1** and poly-(*S*)-**1**—indicating that the secondary structures adopted by the copolymers resemble the structures adopted by the homopolymers (Figure 2b).

Next, stereocomplexation studies were carried out by mixing solutions of the copolymers with the complementary enantiomeric parent homopolymer. For instance, a mixture of poly-[(*R*)-$\mathbf{1}_{0.99}$-*co*-$\mathbf{2}_{0.01}$] (0.1 mg mL^{-1} in THF) with poly-(*S*)-**1** (0.1 mg mL^{-1} in THF) in a 50/50 (v/v) ratio. Thus, six different stereocomplexes were prepared—poly-[(*R*)-$\mathbf{1}_{0.99}$-*co*-$\mathbf{2}_{0.01}$]/poly-(*S*)-**1**; poly-[(*R*)-$\mathbf{1}_{0.98}$-*co*-$\mathbf{2}_{0.02}$]/poly-(*S*)-**1**; poly-[(*R*)-$\mathbf{1}_{0.97}$-*co*-$\mathbf{2}_{0.03}$]/poly-(*S*)-**1** (Figure 2c) and poly-[(*S*)-$\mathbf{1}_{0.99}$-*co*-$\mathbf{2}_{0.01}$]/poly-(*R*)-**1**; poly-[(*S*)-$\mathbf{1}_{0.98}$-*co*-$\mathbf{2}_{0.02}$]/poly-(*R*)-**1**; poly-[(*S*)-$\mathbf{1}_{0.97}$-*co*-$\mathbf{2}_{0.03}$]/poly-(*R*)-**1** (see SI).

In all cases, DLS studies show the presence of large aggregates (Figure 2c and SI), which correspond to fiber-like aggregates as inferred from SEM studies (Figures 2d and SI).

Analogous sterecomplexation studies were carried out between the complementary thiolated copolymers, poly-[(*R*)-$\mathbf{1}_{0.99}$-*co*-$\mathbf{2}_{0.01}$]/poly-[(*S*)-$\mathbf{1}_{0.99}$-*co*-$\mathbf{2}_{0.01}$]; poly-[(*R*)-$\mathbf{1}_{0.98}$-*co*-$\mathbf{2}_{0.02}$]/poly-[(*S*)-$\mathbf{1}_{0.98}$-*co*-$\mathbf{2}_{0.02}$], which produced large aggregates as inferred from DLS and SEM studies (Figure 2c). These stereocomplexes display stimuli-responsive properties, which makes it possible to switch ON/OFF the stereocomplex by playing with the donor character of the solvent and with temperature. Thus, while the donor character of the solvent affects the *cis*/*trans* content of the anilide group and therefore the formation of the stereocomplex—ON (donor solvents, *cis* anilide), OFF (non-donor solvents, *trans* anilide)—(Figure 3), an increase in the temperature of the solution—warming up to 60 °C—of the dispersed stereocomplex promotes disruption of the network of H-bonds that hold the enantiomeric and complementary *cis*-anilide *M* helix and *cis*-anilide *P* helix linked together (Figure 3).

Once the ability of designed copolymers to form stereocomplexes was demonstrated, we proceeded to the preparation of nanocomposites by hybridization with MNPs (M = Au or Ag).

2.1. Poly-[(R)-$\mathbf{1}_{1-r}$-co-$\mathbf{2}_{r}$]-MNPs and Poly-[(S)-$\mathbf{1}_{1-r}$-co-$\mathbf{2}_{r}$]-MNPs Nanocomposites: Dynamic Behavior Studies.

Six different poly-[(*R*)-$\mathbf{1}_{1-r}$-*co*-$\mathbf{2}_{r}$]-MNPs and poly-[(*S*)-$\mathbf{1}_{1-r}$-*co*-$\mathbf{2}_{r}$]-MNPs nanocomposites (r = 0.01−0.03; M = Au and Ag) were prepared following a variation of the classical Brust-Schiffrin procedure (see SI for synthetic details). ECD studies of THF solutions of poly-[(*R*)-$\mathbf{1}_{1-r}$-*co*-$\mathbf{2}_{r}$]-MNPs and poly-[(*S*)-$\mathbf{1}_{1-r}$-*co*-$\mathbf{2}_{r}$]-MNPs (0.3 mg mL^{-1}) showed an active Cotton Effect in the vinylic region (ca. 380 nm) indicating that the nanocomposites retain the helical structure of Poly-**1** when the MNPs are hybridized (Figure 4 and SI). Moreover, UV−vis studies of the nanocomposites confirmed the formation of MNPs where AgNPs showed the typical LSPR band at 420 nm, associated with the yellowish color of the poly-[(*R*)-$\mathbf{1}_{1-r}$-*co*-$\mathbf{2}_{r}$]-AgNPs and poly-[(*S*)-$\mathbf{1}_{1-r}$-*co*-$\mathbf{2}_{r}$]-AgNPs solutions. Moreover, AuNPs showed the LSPR band at 530 nm associated with the reddish color of the poly-[(*R*)-$\mathbf{1}_{1-r}$-*co*-$\mathbf{2}_{r}$]-AuNPs and poly-[(*S*)-$\mathbf{1}_{1-r}$-*co*-$\mathbf{2}_{r}$]-AuNPs solutions (Figure 4 and SI).

TEM studies were carried out to study the morphology of the MNPs within the nanocomposites which revealed the formation of low polydisperse spherical AuNPs (7.1 ± 3.3 nm) and AgNPs (4.4 ± 1.5 nm) (Figure 4d,h). These nanocomposites are stable for several weeks dispersed in solution and the solid state, a fact that indicates the key role of poly-

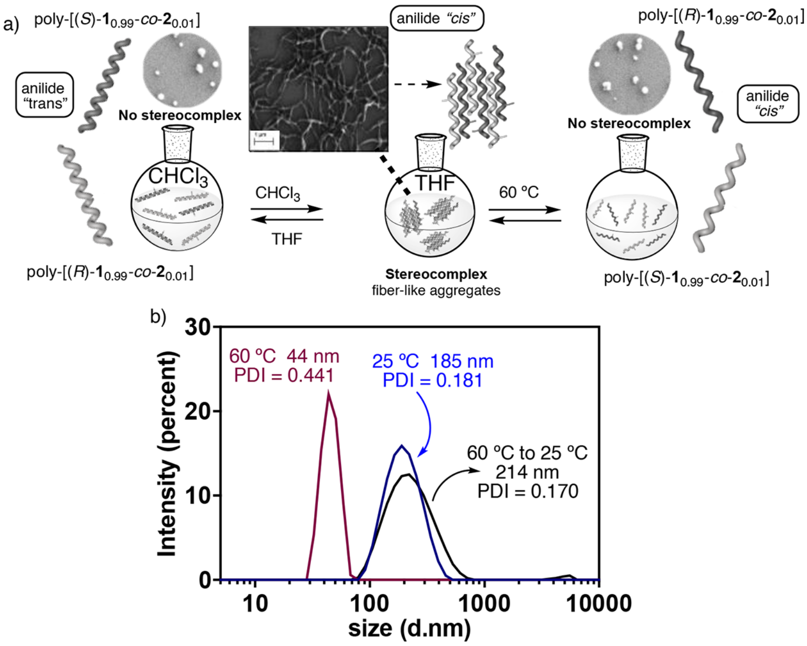

Figure 3. (a) Graphic illustration and electron microscopy studies of the ON/OFF stereocomplexation of a 50/50 v/v mixture of poly-[(R)-$\mathbf{1}_{0.98}$-co-$\mathbf{2}_{0.02}$]/poly-[(S)-$\mathbf{1}_{0.98}$-co-$\mathbf{2}_{0.02}$] in $CHCl_3$ (OFF), THF (ON) and THF at 60 °C (OFF). (b) DLS studies of the ON/OFF stereocomplexation of a 50/50 (v/v) mixture of poly-[(R)-$\mathbf{1}_{0.98}$-co-$\mathbf{2}_{0.02}$]/ poly-[(S)-$\mathbf{1}_{0.98}$-co-$\mathbf{2}_{0.02}$] in THF (ON), THF at 60 °C (OFF) and cooling again to 25 °C (scale bar stereocomplex: 1000 nm).

[(R)-$\mathbf{1}_{1-r}$-co-$\mathbf{2}_r$] and poly-[(S)-$\mathbf{1}_{1-r}$-co-$\mathbf{2}_r$] (r = 0.01−0.03) in the stabilization of the MNPs.

Moreover, ECD and UV−vis studies of poly-[(R)-$\mathbf{1}_{1-r}$-co-$\mathbf{2}_r$]-MNPs and poly-[(S)-$\mathbf{1}_{1-r}$-co-$\mathbf{2}_r$]-MNPs nanocomposites (M = Au or Ag) in different solvents—$CHCl_3$, DCM, DMF, and DMSO—showed the formation of dynamic helical copolymers-MNPs nanocomposites with behavior like that of the parent homopolymer Poly-**1** (see SI). Hence, it is possible to obtain nanocomposites with a chiral dynamic *P*/*M* coating by tuning the polar/donor properties of the solutions of poly-[(R)-$\mathbf{1}_{1-r}$-co-$\mathbf{2}_r$]-MNPs and poly-[(S)-$\mathbf{1}_{1-r}$-co-$\mathbf{2}_r$]-MNPs nanocomposites (see SI).

2.2. Stereocomplexation of PPA-Nanocomposites: Stimuli-Responsive Properties. Once the formation of the nanocomposites was demonstrated, the next step consisted in the preparation of the different stereocomplexes. The preparation of a dynamic stereocomplex nanocomposite is not straightforward. It is necessary to design a copolymer that meets three requirements: (1) the stabilization of the metallic nanoparticle, (2) the ability to form enantiomeric and complementary helices to induce the stereocomplex, and (3) the possibility of tuning the helical structure by external stimuli to create a stereocomplex switch (ON/OFF) of the nanocomposites.

To determine if our system comprises these requirements and is able to create a dynamic stereocomplex nanocomposite, we first explore the stereocomplexation between a nanocomposite and the complementary homopolymers. For this purpose, mixtures of the hybrid material (0.3 mg mL^{-1}, THF) with the enantiomeric homopolymer (0.3 mg mL^{-1}, THF) in a 50/50 (v/v) mixture were prepared. As a result, the following mixtures were made: poly-[(R)-$\mathbf{1}_{1-r}$-co-$\mathbf{2}_r$]-AgNPs/poly-(S)-**1**; poly-[(R)-$\mathbf{1}_{1-r}$-co-$\mathbf{2}_r$]-AuNPs/poly-(S)-**1**; poly-[(S)-$\mathbf{1}_{1-r}$-co-$\mathbf{2}_r$]-AgNPs/poly-(R)-**1**; poly-[(R)-$\mathbf{1}_{1-r}$-co-$\mathbf{2}_r$]-AgNPs/poly-(R)-**1** (r = 0.01−0.03). In addition, another family of stereocomplexes were prepared by mixing two nanocomposites containing complementary enantiomeric helical structures hybridized to the same or different metal nanoparticle, i.e., poly-[(R)-$\mathbf{1}_{0.98}$-co-$\mathbf{2}_{0.02}$]-AuNPs/poly-[(S)-$\mathbf{1}_{0.98}$-co-$\mathbf{2}_{0.02}$]-AgNPs; poly-[(R)-$\mathbf{1}_{0.99}$-co-$\mathbf{2}_{0.1}$]-AuNPs/poly-[(S)-$\mathbf{1}_{0.99}$-co-$\mathbf{2}_{0.01}$]-AgNPs; poly-[(R)-$\mathbf{1}_{0.98}$-co-$\mathbf{2}_{0.02}$]-AuNPs/poly-[(S)-$\mathbf{1}_{0.97}$-co-$\mathbf{2}_{0.03}$]-AgNPs; poly-[(R)-**1**/poly-[(S)-$\mathbf{1}_{0.98}$-co-$\mathbf{2}_{0.02}$]-AuNPs (see SI for more details.).

DLS studies showed in all cases the presence of larger aggregates, which was corroborated by electron microscopy studies—SEM, TEM—(Figure 5a,b and SI) that indicated the presence of fiber-like aggregates where the MNPs are distributed in the entire fibrillar structure. From these studies, it was found that the MNP attached to a dynamic PPA copolymer does not affect its structure or its stereocomplexation ability.

Next, stimuli-responsive studies were carried out with the different stereocomplex-nanocomposites to determine if it is possible to control the formation/disruption (ON/OFF) of the stereocomplex by altering the secondary structure of the polymer, or by activating/deactivating the network of H-bonds that keep the stereocomplex nanocomposite linked together.

As expected, it was found that by playing with the donor character of the solvent it is possible to switch ON (THF)/OFF (chloroform) the stereocomplex-nanocomposite (Figure 5a,b and SI). The same switch was obtained in a stereocomplex-nanocomposite dispersed in THF by playing with the temperature—ON (<60 °C)/OFF (>60 °C)—(Figure 5c,d and SI).

3. CONCLUSIONS

In this work, it was demonstrated that it is possible to prepare stimuli-responsive stereocomplex-nanocomposites based on dynamic-helical polymer-MNP (M = Au or Ag) hybrid materials. Thus, two complementary and enantiomeric helical polymers functionalized with Au or Ag nanoparticles interact

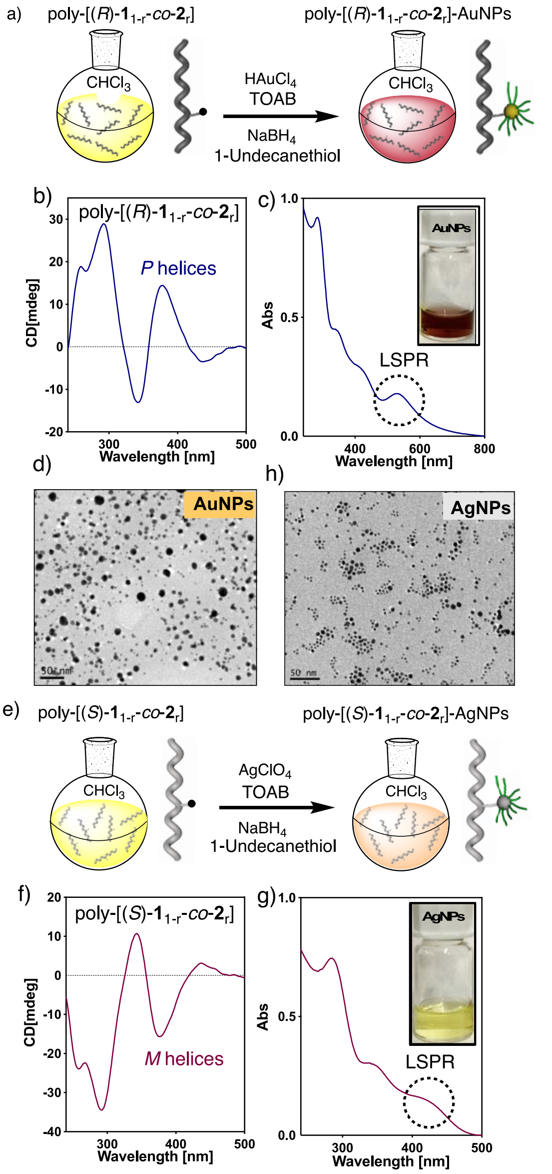

Figure 4. (a) Graphic illustration for the preparation of poly-[(R)-$\mathbf{1}_{1-r}$-co-$\mathbf{2}_r$]-AuNPs. (b) CD spectrum of poly-[(R)-$\mathbf{1}_{0.99}$-co-$\mathbf{2}_{0.01}$]-AuNPs. (c) UV−vis spectrum of poly-[(R)-$\mathbf{1}_{0.99}$-co-$\mathbf{2}_{0.01}$]-AuNPs. (d) TEM image of poly-[(R)-$\mathbf{1}_{0.99}$-co-$\mathbf{2}_{0.01}$]-AuNPs (scale bar: 50 nm). (e) Graphic illustration for the preparation of poly-[(S)-$\mathbf{1}_{0.99}$-co-$\mathbf{2}_{0.01}$]-AgNPs. (f) CD spectrum of poly-[(S)-$\mathbf{1}_{0.99}$-co-$\mathbf{2}_{0.01}$]-AgNPs. (g) UV−vis spectrum of poly-[(S)-$\mathbf{1}_{0.99}$-co-$\mathbf{2}_{0.01}$]-AgNPs. (h) TEM image of poly-[(S)-$\mathbf{1}_{0.99}$-co-$\mathbf{2}_{0.1}$]-AgNPs (scale bar: 50 nm).

between them to form fiber-like aggregates stabilized by a hydrogen bonding network formed by *cis*-amide groups located at the crest of the helical polymers. The possibility of tuning the helical structure of the polymer by external stimuli in combination with the possibility of acting on the hydrogen bonding network makes it possible to create a stimulus-responsive stereocomplex nanocomposite, and where different fiber-like nanostructures can be obtained for the mixture of enantiomeric hybrid materials.

This work is pioneering in this topic, and we believe that important applications can emerge both in the field of helical polymers and in the field of metal nanoparticles by a correct design of the hybrid materials used to prepare the stereocomplexes.

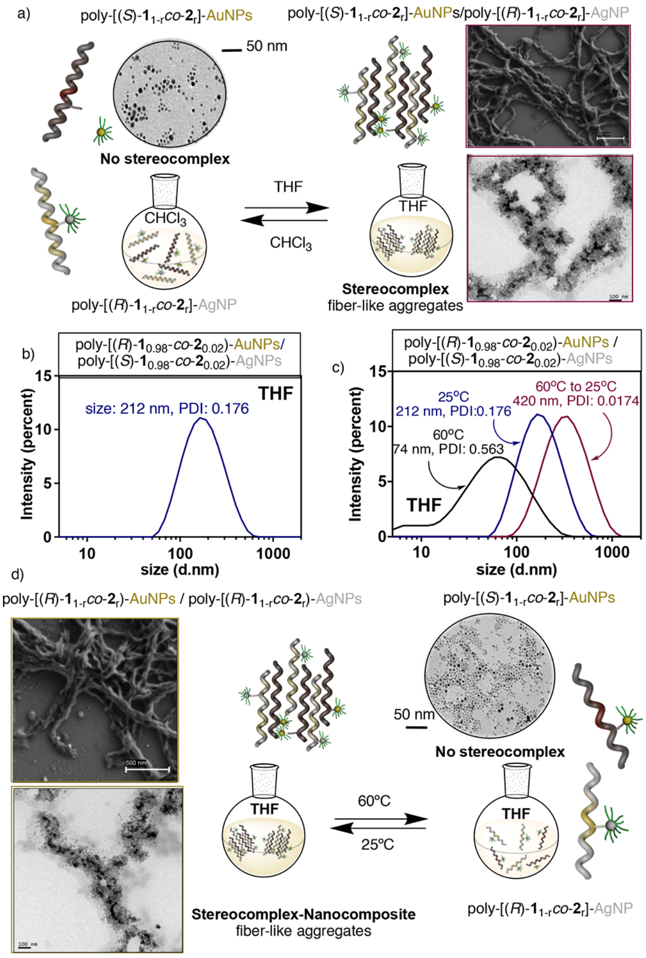

Figure 5. (a) Graphic illustration and electron microscopy studies of the ON/OFF stereocomplexation-nanocomposite of a 50/50 v/v mixture of poly-[(R)-$\mathbf{1}_{0.98}$-co-$\mathbf{2}_{0.02}$]-AgNP/poly-[(S)-$\mathbf{1}_{0.98}$-co-$\mathbf{2}_{0.02}$]-AuNP nanocomposites in $CHCl_3$ (OFF) and THF (ON). (b) DLS studies of the ON/OFF stereocomplexation of a 50/50 (v/v) mixture of poly-[(R)-$\mathbf{1}_{0.98}$-co-$\mathbf{2}_{0.02}$]-AgNP/ poly-[(S)-$\mathbf{1}_{0.98}$-co-$\mathbf{2}_{0.02}$]-AuNP nanocomposites in THF (ON) and $CHCl_3$ (OFF). (c) Reversible stereocomplex-nanocomposite formation of a 50/50 (v/v) mixture of poly-[(R)-$\mathbf{1}_{0.98}$-co-$\mathbf{2}_{0.02}$]-AgNP/ poly-[(S)-$\mathbf{1}_{0.98}$-co-$\mathbf{2}_{0.02}$]-AuNP nanocomposites in THF mediated by temperature changes. (d) Graphic illustration and electron microscopy studies of the ON/OFF stereocomplexation-nanocomposite of a 50/50 v/v mixture of poly-[(R)-$\mathbf{1}_{1-r}$-co-$\mathbf{2}_r$]-AgNP/poly-[(S)-$\mathbf{1}_{1-r}$-co-$\mathbf{2}_r$]-AuNP nanocomposites in THF mediated by temperature changes.

4. EXPERIMENTAL SECTION

4.1. Chemicals. Commercially available chemicals have been used as delivered. Solvents were purchased as reagent grade and distilled if necessary. Anhydrous solvents were either purchased as ultra-dry solvents from Acros Organics or received from a solvent purification system. For the coupling and polymerization reactions, dry THF was obtained from the MBRAUN SPS 800 solvent purification system. Water was purified by the Millipore water purification system. Coupling reagents (2-(7-Aza-1H-benzotriazole-1-yl)-1,1,3,3-tetramethyluronium hexafluorophosphate) (HATU), 4-ethynylbenzoic acid, and 4-ethynylaniline were purchased from AnaSpec Inc. (R)-(S)-α-methoxy-α-trifluoromethylphenylacetic acid, 11-mercaptoundecanoic acid, oxalyl chloride, rhodium norbornadiene chloride dimer {[Rh(*nbd*)Cl]$_2$}, diisopropyltriethylamine (DIEA), triethylamine (TEA, 99%), 1-dodecanethiol, sodium borohydride ($NaBH_4$), gold(III) chloride trihydrate ($HAuCl_4$) and silver perchlorate ($AgClO_4$) were purchased from Aldrich.

4.2. Instrumentations and Characterizations. NMR experiments were carried out in a Varian Inova 300 (300 MHz resonance 1H). Size exclusion chromatography studies were performed on the Alliance 2695 HPLC System (Waters) liquid chromatography system equipped with a UV 2489 detector (Waters). The samples were eluted by three Phenogel columns connected to each other with stationary phases of 10^3, 10^4, and 10^5 Amstrong and packed with a solid support of a cross-linked styrene and *p*-divinylbenzene copolymer. CD and UV measurements were registered in a Jasco-720 spectropolarimeter and a Jasco-730 spectrophotometer respectively at a nanocomposite concentration of 0.3 mg mL^{-1}. FT-IR measurements were carried out on a Bruker IFS-66v. DLS studies were performed on a Nano-ZS 90 (Malvern) equipped with a He-Ne laser (l = 633 nm) under a scattering angle of 173°. The samples were maintained at the designed temperature for 5 min before testing. DLS measurements were carried out in all cases at 0.1 mg·mL^{-1}. SEM measurements were performed on an LEO-435VP electron microscope equipped with an energy-dispersive X-ray (EDX) spectrometer. TEM measurements were performed on a JEOL JEM 2010 and 200 KV as a voltage. To study the nanocomposites or stereocomplexes, the same protocol was used. A dispersion of the nanocomposites or stereocomplexes at a concentration of 0.1 mg mL^{-1} was drop-casted onto of silicon wafer chip and allowed to dry at rt for 12 h for SEM studies, while in the case of TEM studies, the dispersed materials were drop-casted onto a carbon chip and allowed to dry at rt for 12 h.

ASSOCIATED CONTENT

Supporting Information

The Supporting Information is available free of charge at https://pubs.acs.org/doi/10.1021/acs.chemmater.3c00912.

Materials and methods, synthesis of monomers, synthesis of copolymers, thermal studies for copolymers, TGA studies, CD studies of poly-($\mathbf{1}_{1-r}$-*co*-2_r) (r = 0.01−0.03) in different solvents, aggregation studies for copolymers poly-($\mathbf{1}_{1-r}$-*co*-2_r) series, SEM microscopy images for sterocomplexes formed by copolymers poly-[$\mathbf{1}_{1-r}$-*co*-2_r] (r = 0.01−0.03), synthesis of poly-($\mathbf{1}_{1-r}$-*co*-2_r)-AuNPs and poly-($\mathbf{1}_{1-r}$-*co*-2_r)-AgNPs (r = 0.01−0.03), stimuli-responsive studies of poly-($\mathbf{1}_{1-r}$-*co*-2_r)-MNPs (M = Au or Ag) in different solvents, Raman studies of poly-($\mathbf{1}_{1-r}$-*co*-2_r)-MNPs (Au or Ag), Raman studies of poly-($\mathbf{1}_{1-r}$-*co*-2_r)-MNPs (Au or Ag), ON/OFF stereocomplexation studies of copolymers poly-[(R)-$\mathbf{1}_{1-r}$-*co*-2_r)]/poly-[(S)-$\mathbf{1}_{1-r}$-*co*-2_r)] and poly-($\mathbf{1}_{1-r}$-*co*-2_r)/poly-1, CD studies of copolymers poly-($\mathbf{1}_{1-r}$-*co*-2_r)-MPNs (M = Au or Ag), aggregation studies for copolymers poly-($\mathbf{1}_{1-r}$-*co*-2_r)-MPNs (M = Au or Ag), SEM studies of poly-[(R)-$\mathbf{1}_{1-r}$-*co*-2_r)]/poly-[(S)-$\mathbf{1}_{1-r}$-*co*-2_r)]-MNPs mixtures, TEM studies of poly-[(R)-$\mathbf{1}_{1-r}$-*co*-2_r)]-AuNPs/poly-[(S)-$\mathbf{1}_{1-r}$-*co*-2_r)]-AgNPs mixtures, and references (PDF)

AUTHOR INFORMATION

Corresponding Author

Félix Freire − *Centro Singular de Investigación en Química Biolóxica e Materiais Moleculares (CiQUS), Universidade de Santiago de Compostela, 15782 Santiago de Compostela, Spain*; orcid.org/0000-0002-2672-5830;
Email: felix.freire@usc.es

Authors

Manuel Núñez-Martínez − *Centro Singular de Investigación en Química Biolóxica e Materiais Moleculares (CiQUS), Universidade de Santiago de Compostela, 15782 Santiago de Compostela, Spain*

Emilio Quiñoá − *Centro Singular de Investigación en Química Biolóxica e Materiais Moleculares (CiQUS), Universidade de Santiago de Compostela, 15782 Santiago de Compostela, Spain*; orcid.org/0000-0003-3019-3408

Complete contact information is available at:
https://pubs.acs.org/10.1021/acs.chemmater.3c00912

Author Contributions

The manuscript was written through contributions of all authors. All authors have given approval to the final version of the manuscript.

Funding

Financial support from AEI (PID2019-109733GB-I00), Xunta de Galicia (ED431C 2022/21, Centro Singular de Investigación de Galicia acreditación 2019−2022, ED431G 2019/03, and the European Regional Development Fund (ERDF) and is gratefully acknowledged.

Notes

The authors declare no competing financial interest.

ACKNOWLEDGMENTS

M. N.-M. thanks MICINN for a FPI contract (BES-2016-078107). We also thank Servicio de Microscopía Electrónica (RIAIDT, Universidad de Santiago de Compostela) for SEM and TEM studies.

REFERENCES

(1) Dreaden, E.; Alkilany, A.; Huang, X.; Murphy, C.; El-Sayed, M. The golden age: gold nanoparticles for biomedicine. *Chem. Soc. Rev.* **2012**, *41*, 2740−2779.

(2) Jaque, D.; Martínez Maestro, L.; del Rosal, B.; Haro-Gonzalez, P.; Benayas, A.; Plaza, J.; Martín Rodriguez, E.; García Solé, J. Nanoparticles for photothermal therapies. *Nanoscale* **2014**, *6*, 9494−9530.

(3) Zhang, S.; Geryak, R.; Geldmeier, J.; Kim, S.; Tsukruk, V. Synthesis, Assembly, and Applications of Hybrid Nanostructures for Biosensing. *Chem. Rev.* **2017**, *117*, 12942−13038.

(4) Moon, H.; Kim, Y. Fluorescent Polyethylene by In Situ Facile Synthesis of Carbon Quantum Dots Facilitated by Silica Nanoparticle Agglomerates. *ACS Appl. Polym. Mater.* **2021**, *3*, 2768−2775.

(5) Schrinner, M.; Ballauff, M.; Talmon, Y.; Kauffmann, Y.; Thun, J.; Moller, M.; Breu, J. Single Nanocrystals of Platinum Prepared by Partial Dissolution of Au-Pt Nanoalloys. *Science* **2009**, *323*, 617.

(6) González-Rubio, G.; Mosquera, J.; Kumar, V.; Pedrazo-Tardajos, A.; Llombart, P.; Solís, D. M.; Lobato, I.; Noya, E. G.; Guerrero-Martínez, A.; Taboada, J. M.; Obelleiro, F.; MacDowell, L. G.; Bals, S.; Liz-Marzán, L. M. Micelle-directed chiral seeded growth on anisotropic gold nanocrystals. *Science* **2020**, *368*, 1472−1477.

(7) Bergueiro, J.; Núñez-Martínez, M.; Arias, S.; Quiñoá, E.; Riguera, R.; Freire, F. Chiral gold−PPA nanocomposites with tunable helical sense and morphology. *Nanoscale Horiz.* **2020**, *5*, 495−500.

(8) Núñez-Martínez, M.; Arias, S.; Quiñoá, E.; Riguera, R.; Freire, F. Dynamic Chiral PPA−AgNP Nanocomposites: Aligned Silver Nanoparticles Decorating Helical Polymers. *Chem. Mater.* **2021**, *33*, 4805−4812.

(9) Núñez-Martínez, M.; Arias, S.; Bergueiro, J.; Quiñoá, E.; Riguera, R.; Freire, F. The Role of Polymer−AuNP Interaction in the Stimuli-Response Properties of PPA−AuNP Nanocomposites. *Macromol. Rapid Commun.* **2022**, *43*, No. 2270009.

(10) Núñez-Martínez, M.; Quiñoá, E.; Freire, F. Chiroptical and colorimetric switches based on helical polymer-metal nanocomposites prepared *via* redox metal translocation of helical polymer metal complexes. *Nanoscale* **2022**, *14*, 13066−13072.

(11) Wang, S.; Chen, J.; Feng, X.; Shi, G.; Zhang, J.; Wan, X. Conformation Shift Switches the Chiral Amplification of Helical

Copoly(phenylacetylene)s from Abnormal to Normal "Sergeants-and-Soldiers" Effect. *Macromolecules* **2017**, *50*, 4610−4615.

(12) Freire, F.; Quiñoá, E.; Riguera, R. Supramolecular Assemblies from Poly(phenylacetylene)s. *Chem. Rev.* **2016**, *116*, 1242−1271.

(13) Freire, F.; Seco, J. M.; Quiñoá, E.; Riguera, R. Helical polymer−metal complexes: the role of metal ions on the helicity and the supramolecular architecture of poly (phenylacetylene) s. *Adv. Polym. Sci.* **2013**, *262*, 123−140.

(14) Yashima, E. Synthesis and structure determination of helical polymers. *Polym. J.* **2010**, *42*, 3−16.

(15) Yashima, E.; Maeda, K. Chirality-Responsive Helical Polymers. *Macromolecules* **2008**, *41*, 3−12.

(16) Percec, V.; Rudick, J. G.; Peterca, M.; Heiney, P. A. Nanomechanical Function from Self-Organizable Dendronized Helical Polyphenylacetylenes. *J. Am. Chem. Soc.* **2008**, *130*, 7503−7508.

(17) Arias, S.; Núñez-Martinez, M.; Quiñoá, E.; Riguera, R.; Freire, F. A general route to chiral nanostructures from helical polymers: *P*/*M* switch *via* dynamic metal coordination. *Polym. Chem.* **2017**, *8*, 3740−3745.

(18) Suárez-Picado, E.; Quiñoá, E.; Riguera, R.; Freire, F. Poly(phenylacetylene) Amines: A General Route to Water-Soluble Helical Polyamines. *Chem. Mater.* **2018**, *30*, 6908−6914.

(19) Rodríguez, R.; Suárez-Picado, E.; Quiñoá, E.; Riguera, R.; Freire, F. A Stimuli-Responsive Macromolecular Gear: Interlocking Dynamic Helical Polymers with Foldamers. *Angew. Chem., Int. Ed.* **2020**, *59*, 8616−8622.

(20) Suárez-Picado, E.; Quiñoá, E.; Riguera, R.; Freire, F. Chiral Overpass Induction in Dynamic Helical Polymers Bearing Pendant Groups with Two Chiral Centers. *Angew. Chem., Int. Ed.* **2020**, *59*, 4537−4543.

(21) Fernández, Z.; Fernández, B.; Quiñoá, E.; Riguera, R.; Freire, F. Chiral information harvesting in helical poly(acetylene) derivatives using oligo(*p*-phenyleneethynylene)s as spacers. *Chem. Sci.* **2020**, *11*, 7182−7187.

(22) Rodríguez, R.; Quiñoá, E.; Riguera, R.; Freire, F. Multistate Chiroptical Switch Triggered by Stimuli-Responsive Chiral Teleinduction. *Chem. Mater.* **2018**, *30*, 2493−2497.

(23) Rodríguez, R.; Quiñoá, E.; Riguera, R.; Freire, F. Architecture of Chiral Poly(phenylacetylene)s: From Compressed/Highly Dynamic to Stretched/Quasi-Static Helices. *J. Am. Chem. Soc.* **2016**, *138*, 9260−9628.

(24) Freire, F.; Seco, J. M.; Quiñoá, E.; Riguera, R. Nanospheres with Tunable Size and Chirality from Helical Polymer−Metal Complexes. *J. Am. Chem. Soc.* **2012**, *134*, 19374−19383.

(25) Arias, S.; Núñez-Martínez, M.; Quiñoá, E.; Riguera, R.; Freire, F. Simultaneous Adjustment of Size and Helical Sense of Chiral Nanospheres and Nanotubes Derived from an Axially Racemic Poly(phenylacetylene). *Small* **2017**, *13*, No. 1602398.

(26) Rey-Tarrío, F.; Guisán-Ceinos, S.; Cuerva, J.; Miguel, D.; Ribagorda, M.; Quiñoá, E.; Freire, F. Photostability and Dynamic Helical Behavior in Chiral Poly(phenylacetylene)s with a Preferred Screw-Sense. *Angew. Chem., Int. Ed.* **2022**, *61*, No. e202207623.

(27) Tarrío, J. J.; Rodríguez, R.; Fernández, B.; Quiñoá, E.; Freire, F. Dissymmetric Chiral Poly(diphenylacetylene)s: Secondary Structure Elucidation and Dynamic Luminescence. *Angew. Chem., Int. Ed.* **2022**, *61*, No. e202115070.

(28) Ishidate, R.; Markvoort, A. J.; Maeda, K.; Yashima, E. Unexpectedly Strong Chiral Amplification of Chiral/Achiral and Chiral/Chiral Copolymers of Biphenylylacetylenes and Further Enhancement/Inversion and Memory of the Macromolecular Helicity. *J. Am. Chem. Soc.* **2019**, *141*, 7605−7614.

(29) Yashima, E.; Ousaka, N.; Taura, D.; Shimomura, K.; Ikai, T.; Maeda, K. Supramolecular Helical Systems: Helical Assemblies of Small Molecules, Foldamers, and Polymers with Chiral Amplification and Their Functions. *Chem. Rev.* **2022**, *116*, 13752−13990.

(30) Ikai, T.; Okuda, S.; Aizawa, M.; Yashima, E. Catalytic One-Handed Helix Induction and Subsequent Static Memory of Poly(biphenylylacetylene)s Assisted by a Small Amount of Carboxy Groups Introduced at the Pendants. *ACS Macro Lett.* **2022**, *11*, 525−531.

(31) Echizen, K.; Taniguchi, T.; Nishimura, T.; Maeda, K. Well-Controlled Living Polymerization of Phenylacetylenes in Water: Synthesis of Water-Soluble Stereoregular Telechelic Poly(phenylacetylene)s. *Angew. Chem., Int. Ed.* **2022**, *61*, No. e202282662.

(32) Yan-Xiang, L.; Lei, X.; Shu-Ming, K.; Li, Z.; Na, L.; Zong-Quan, W. Helicity- and Molecular-Weight-Driven Self-Sorting and Assembly of Helical Polymers towards Two-Dimensional Smectic Architectures and Selectively Adhesive Gels. *Angew. Chem., Int. Ed.* **2021**, *60*, 7174−7179.

(33) Zhou, L.; Chong-Long, L.; Run-Tan, G.; Shu-Ming, K.; Lei, X.; Xun-Hui, X.; Liu, N.; Zong-Quan, W. Highly Regioselective and Helix-Sense Selective Living Polymerization of Phenyl and Alkoxyallene Using Chiral Nickel(II) Catalysts. *Macromolecules* **2021**, *54*, 679−686.

(34) Xu, X.; Kang, S.; Gao, R.; Chen, Z.; Liu, N.; Wu, Z.-Q. Precise Synthesis of Optically Active and Thermo-degradable Poly(trifluoromethyl methylene) with Circularly Polarized Luminescence. *Angew. Chem., Int. Ed.* **2023**, *62*, No. e202300882.

(35) Xu, L.; Wu, Y.; Gao, R.; Li, S.; Liu, N.; Wu, Z. Visible Helicity Induction and Memory in Polyallene toward Circularly Polarized Luminescence, Helicity Discrimination, and Enantiomer Separation. *Angew. Chem., Int. Ed.* **2023**, *62*, No. e202217234.

(36) Wu, Z.; Song, X.; Li, Y.; Zhou, L.; Zhu, Y.; Chen, Z.; Liu, N. Achiral organoiodine-functionalized helical polyisocyanides for multiple asymmetric dearomative oxidations. *Nat. Commun.* **2023**, *14*, 566.

(37) Liu, N.; Zhou, L.; Wu, Z. Alkyne-Palladium(II)-Catalyzed Living Polymerization of Isocyanides: An Exploration of Diverse Structures and Functions. *Acc. Chem. Res.* **2021**, *54*, 3953−3967.

(38) Huang, H. H.; Ni, X. P.; Loy, G. L.; Chew, C. H.; Tan, K. L.; Loh, F. C.; Deng, J. F.; Xu, G. Q. Photochemical Formation of Silver Nanoparticles in Poly(*N*-vinylpyrrolidone). *Langmuir* **1996**, *12*, 909−912.

(39) Zhang, Z.; Zhao, B.; Hu, L. PVP Protective Mechanism of Ultrafine Silver Powder Synthesized by Chemical Reduction Processes. *J. Solid State Chem.* **1996**, *121*, 105−110.

(40) Zhang, G.; Bao, Y.; Pan, M.; Wang, N.; Cheng, X.; Zhang, W. Memorable full-color circularly polarized luminescence from chiral co-assembled polymer films enabled by multipath transfer. *Sci. China: Chem.* **2023**, *66*, 1169−1178.

(41) Zhang, G.; Cheng, X.; Wang, Y.; Zhang, W. Supramolecular chiral polymeric aggregates: Construction and applications. *Aggregate* **2023**, *4*, No. e262.

(42) Fittolani, G.; Seeberger, P.; Delbianco, M. Helical polysaccharides. *Pept. Sci.* **2020**, *112*, No. e24124.

(43) Slagen, J.; Domb, A. Biopolymer stereocomplexes. *Adv. Drug Delivery Rev.* **2003**, *55*, 549−583.

(44) Bertin, A. Emergence of Polymer Stereocomplexes for Biomedical Applications. *Macromol. Chem. Phys.* **2012**, *213*, 2329−2352.

(45) Zhang, G.; Liang, Y.; Wang, Y.; Li, Q.; Qi, W.; Zhang, W.; Su, R.; He, Z. Chirality-Dependent Copper−Diphenylalanine Assemblies with Tough Layered Structure and Enhanced Catalytic Performance. *ACS Nano* **2022**, *16*, 6866−6877.

(46) Sun, Y.; He, C. Synthesis and Stereocomplex Crystallization of Poly(lactide)-Graphene Oxide Nanocomposites. *ACS Macro Lett.* **2012**, *1*, 709−713.

(47) Oberhauser, W.; Evangelisti, C.; Jumde, R.; Petrucci, G.; Bartoli, M.; Frediani, M.; Mannini, M.; Capozzoli, M.; Passaglia, E.; Rosi, L. Palladium-nanoparticles on end-functionalized poly(lactic acid)-based stereocomplexes for the chemoselective cinnamaldehyde hydrogenation: Effect of the end-group. *J. Catal.* **2015**, *330*, 187−196.

(48) Kawauchi, T.; Kitaura, A.; Kumaki, J.; Kusanagi, H.; Yashima, E. Helix-Sense-Controlled Synthesis of Optically Active Poly(methyl methacrylate) Stereocomplexes. *J. Am. Chem. Soc.* **2008**, *130*, 11889−11891.

(49) Kumaki, J.; Kawauchi, T.; Okoshi, K.; Kusanagi, H.; Yashima, E. Supramolecular Helical Structure of the Stereocomplex Composed

of Complementary Isotactic and Syndiotactic Poly(methyl methacrylate)s as Revealed by Atomic Force Microscopy. *Angew. Chem., Int. Ed.* **2007**, *46*, 5348−5351.

(50) Sun, Y.; He, C. Synthesis, stereocomplex crystallization, morphology and mechanical property of poly(lactide)−carbon nanotube nanocomposites. *RSC Adv.* **2013**, *3*, 2219−2226.

(51) Leiras, S.; Freire, F.; Seco, J. M.; Quiñoá, E.; Riguera, R. Reversible assembly of enantiomeric helical polymers: from fibers to gels. *Chem. Sci.* **2015**, *6*, 246−253.